ISBN: 978-3-95450-227-1 ISSN: 2673-5490 doi:10.18429/JACoW-IPAC2022-MOPOTK039

IRON YOKE EFFECTS IN QUADRUPOLE MAGNETS FOR HIGH RIGIDITY ISOTOPE BEAMS*

D.Greene[1†], Y. Choi[1], J. DeKamp[1], S. Manikonda[2], P. Ostroumov[1], M. Portillo[1], J. Wenstrom[1], T. Xu[1]
Facility for Rare Isotope Beams, Michigan State University, East Lansing, USA
Advanced Magnet Lab Inc., Melbourne, USA

Abstract

Iron-dominated superconducting magnets are one of the most popular and most used design choices for superconducting magnetic quadrupoles for accelerator systems. While the iron yoke and pole tips are economic and effective in shaping the field, the large amount of iron also leads to certain drawbacks, namely, unwanted harmonics from the sextupole correctors nested inside of the quadrupole. Additional problems include the nonlinear field profile present in the high-field regime engendered by the presence of steel, and the mechanical and cryogenic design challenges of the entire iron yoke being part of the cold mass. The presented work discusses these effects and challenges by comparing an iron-dominated quadrupole model to an equivalent coil-dominated quadrupole model. The comparison of their respective magnetic harmonics, integrated strength, multipole effects, and mechanical challenges demonstrates that the coil-dominated design is a more favorable choice for select accelerator systems.

INTRODUCTION

The Facility for Rare Isotope Beams (FRIB) requires the transport of secodnary rare isotope beams with high emittance and high magnetic rigidity. The magnetic rigidity of the beam can reach as high as 8 Tm. For beams that require large apertures, that is, apertures on the scale of 0.4 m, large iron yokes for the quadrupole magnets are required in order to have sufficient strength and uniformity [1]. A number of issues are introduced when using large iron yokes on this scale. These include cool down that span weeks and difficulties with alignment of the magnet due to transportation or thermal cycles. The primary issue with using iron yokes, in this application is their undesirable interaction with magnetic sextupole correctors. This effect is the main consideration of the work presented.

An iron yoke with four pole tips, for quadrupole coils, interacts with a sextupole inside of the pole tips due to the difference in their symmetry. This interaction generates a non-zero dipole component that causes a deflection of the beam that can be identified from a harmonic analysis [1]. Our group proposes replacing the iron-dominated quads of the FRIB fragment separator with coil-dominated, iron-free quads in order to minimize this effect.

* Work supported by the U.S. Department of Energy Office of Science under Cooperative Agreement DE-SC0000661, US Department of Energy Office of Science, High Energy Physics under Cooperative Agreement award number DE-SC0018362, and Michigan State University.
† greene@frib.msu.edu

QUAD STEEL AND SEXTUPOLE INTERACTION

FRIB's Ferric Superconducting Quadrupole Type-C (FSQC) is one of the primary magnet types used in the second and third stage of FRIB's fragment separator, sextupole model used can be seen in Fig. 1 [1]. For this reason, it is used to study the effect of the interaction between sextupole and the quad steel. The operating parameters of FSQC as well as the other FSQ magnets can be found in Table 1 and Table 2.

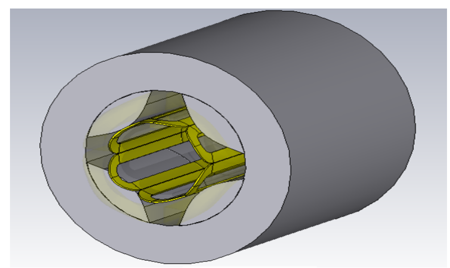

Figure 1: 3D model of FSQC's Sextupole nested inside of the quad iron yoke in CST Studio Suite®.

Table 1: Operating Parameters of FSQA, FSQB, & FSQC [1]

Type	FSQA	FSQB	FSQC
Effective Length (m)	0.723	0.400	0.790
Full Aperture (m)	0.20	0.20	0.20
Max Quad Gradient (T/m)	13.2	17	14
Max Sext. Gradient (T/m^2)	NA	9.6	6.8
Max Oct. Gradient (T/m^3)	NA	48.9	48.5

Table 2: Operating Parameters of FSQD & FSQE [1]

Type	FSQD	FSQE
Effective Length (m)	0.486	0.700
Full Aperture (m)	0.34	0.23
Max Quad Gradient (T/m)	11.9	16.6
Max Sext. Gradient (T/m^2)	NA	NA
Max Oct. Gradient (T/m^3)	NA	NA

Sextupole Field Analysis

The field of FSQC's sextupole was evaluated with CST Studio Suite® with quad coil current at zero. From the field

ISBN: 978-3-95450-227-1 ISSN: 2673-5490 doi:10.18429/JACoW-IPAC2022-MOPOTK039

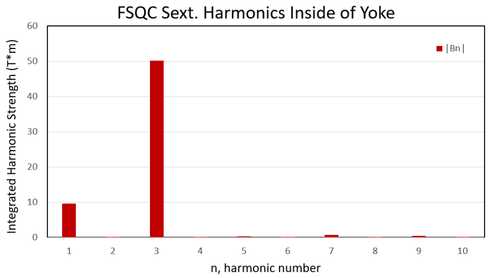

Figure 2: Integrated harmonic decomposition analysis of FSQC Sextupole with inclusion of quadrupole iron yoke [1, 2]. Reference radius of analysis is R=8.1cm from beam axis.

solution, a harmonic decomposition analysis of the field was performed to evaluate the field quality [2].

Figure 2 shows that the highest harmonic present, besides the principle harmonic, is the n=1 dipole harmonic. The dipole harmonic term is about 20% the strength of the principle sextupole term. For an 8 Tm beam, the highest rigidity accessible at FRIB, the integrated dipole term would correspond to a 1.2 milliradian deflection across FSQC.

Optical Analysis

An optical study has been done to determine the effects of this deflection on beam going through a magnet triplet consisting of two FSQB magnets and one FSQC magnet (B-C-B) [1]. Based on the operating parameters and effective length, the FSQB magnets are assumed to contribute about half the deflection of each FSQC.

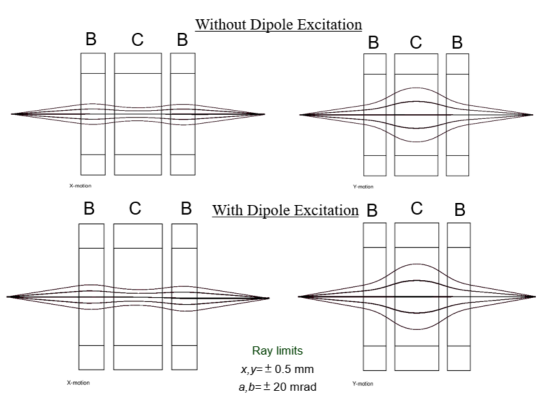

Figure 3: Optics simulation of triplet with a beam rigidity of 8 Tm. The top 2 images are without the inclusion of the dipole harmonic term. The bottom images are the same calculation with the inclusion of the dipole harmonic term. Images in the right column are the dispersive plane and images in left column are the non-dispersive plane. The ray limits refer to the position and momentum range of the ensemble of rays tracked. Letter labelling refers to the corresponding FSQ magnet.

The impact of this deflection can seen in Fig. 3 and more clearly seen when plotted in the phase space and beam center

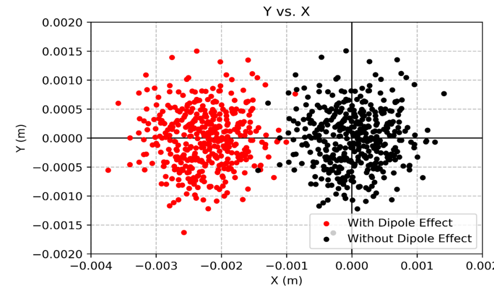

Figure 4: Plot of the X versus Y position for an ensemble of rays tracked through B-C-B triplet comparing results with and without the dipole excitation considered.

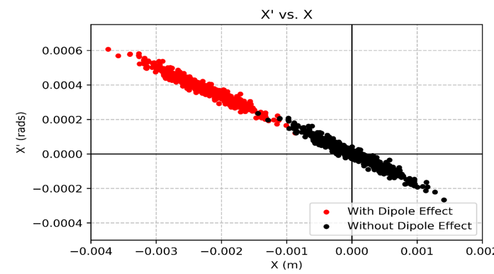

Figure 5: Plot of the X' versus X phase space plot for an ensemble of rays tracked through B-C-B triplet comparing results with and without the dipole excitation considered.

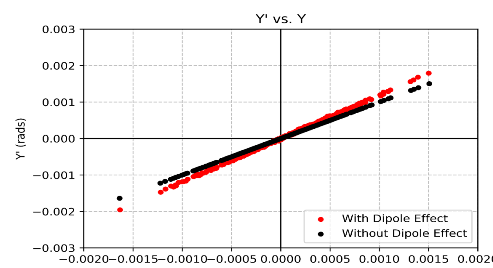

Figure 6: Plot of the Y' versus Y phase space plot for an ensemble of rays tracked through B-C-B triplet comparing results with and without the dipole excitation considered.

through the triplet as shown in Figs. 4, 5 and 6. All ray ensembles were tracked using COSY INFINITY, an arbitrary order beam dynamics simulation and analysis code, and simulated to the second order [3]. Figures 4, 5 and 6 have a Gaussian phase space of ±0.5 mm for X,Y and ±0.02 mrad for X',Y'. The beam center shifts about 2 mm, as shown in Fig. 4.

It is important to point out that these are only the deflection effects through one triplet. The rare isotope beams need to go through 12 FSQB magnets and 4 FSQC magnets in the second and third stage of the fragment separator, as seen in Figs. 7 and 8, where this effect will compound and require some degree of correction.

ISBN: 978-3-95450-227-1 ISSN: 2673-5490 doi:10.18429/JACoW-IPAC2022-MOPOTK039

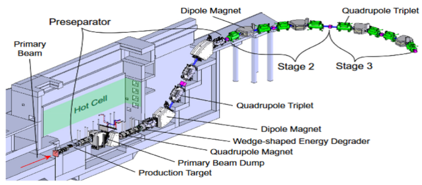

Figure 7: Diagram of the presparator and stage 2 and 3 of FRIB's fragment separator [1].

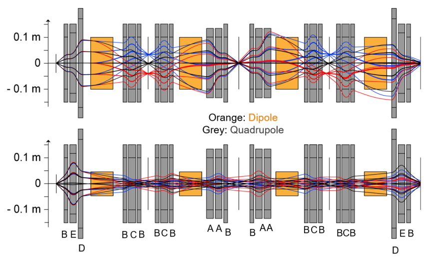

Figure 8: Dispersive (top) and non-dispersive (bottom) plane trajectories through the second and third stages to 5th order approximation. The beam from the pre-separator enters from the left. The angle spread depicted here corresponds to ±31 mrad in X and ±35 mrad in Y and the off-momentum beams shown in red and blue correspond to ±2.3% relative magnetic rigidity [1].

COIL-DOMINATED QUADRUPOLE MODEL

As a solution for the interaction between sextupole and quad steel, we propose coil-dominated quads as an upgrade. Theses quads will be made using the Walstrom method [4,5]. This method allows one to generate coil geometry in which fringe field effects are minimized and higher order harmonic terms are minimized, which enables the creation of high-uniformity quads that do not need the assistance of iron yokes [6, 7].

We have modelled a coil-dominated quadrupole, as seen in Fig. 9, which was designed to perform to the same field specifications as the FSQC quad, as seen in Fig. 10. The field solution of this Walstrom method quadrupole has been simulated in CST Studio Suite®. The quadrupole field of FSQC was also evaluated in CST Studio Suite®. An analysis of each quad's field was carried out, and a comparison was made.

Table 3: Coil-Dominated and FSQC Field Performance Comparison. Reference radius of analysis for each is R=8.1 cm from beam axis.

Parameter	Coil Dominated	FSQC
Amp-Turns (A)	100,800	200,900
Quad Gradient (T/m)	16.79	17.04
Effective Length (m)	0.787	0.782
Non-Uniformity (%)	0.023	0.25
Integrated Strength (T)	13.22	13.34

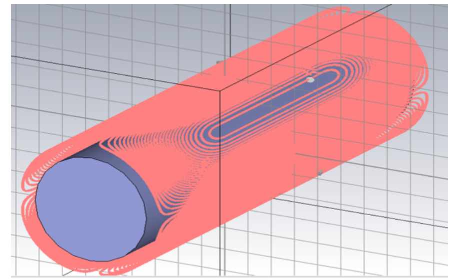

Figure 9: Picture of coil dominated quadrupole 3D model in CST Studio Suite®. Designed to operate to the same field specifications as FSQC. Model is 1.0 m in length.

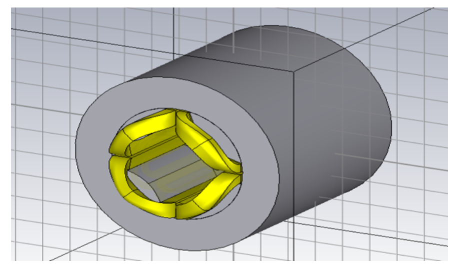

Figure 10: Picture of FSQC quad and iron yoke 3D model in CST Studio Suite®. Quad coils are each 0.9 m in length and the iron yoke is 0.7 m in length.

One can see from Table 3 the coil-dominated model can perform to the same specifications as FSQC with lower non-uniformity, by and order of magnitude, while also being much more compact.

CONCLUSION

Here, we presented a coil-dominated quad design which can perform to the same field specifications as FSQC. Coil-dominated would drastically lower the weight of a triplet by thousands of pounds, reduce cool down time, and reduce the liquid helium inventory. The proposed coil-dominated design would require fewer training quenches than FSQC. The reason for this being that the coil-dominated model would be wound such that the conductor would be placed into paths in a metal bobbin. This means less movement of the conductor is possible than the FSQC quads, which are wound randomly [8]. Finally the coil-dominated quad eliminates the need for any kind of correction due to sextupole interactions with the quad steel. For these reasons, using a coil-dominated model would be an ideal upgrade for select accelerator systems, such as FRIB.

ACKNOWLEDGMENTS

Work supported by the U.S. Department of Energy Office of Science under Cooperative Agreement DE-SC0000661, US Department of Energy Office of Science, High Energy Physics under Cooperative Agreement award number DE-SC0018362, and Michigan State University.

ISBN: 978-3-95450-227-1 ISSN: 2673-5490 doi:10.18429/JACoW-IPAC2022-MOPOTK039

REFERENCES

[1] P. N. Ostorumov *et al.*, "Heavy ion beam physics at Facility for Rare Isotope Beams", *J. Instrum.*, vol. 15, no. 12, pp. 12034-12034, 2020. doi:10.1088/1748-0221/15/12/p12034

[2] S. Russenschuck., *Field Computation for Accelerator Magnets: Analytical and Numerical Methods for Electromagnetic Design and Optimization.*, Wiley-VCH (2011).

[3] M. Berz., "COSY INFINITY reference manual", in *Lawrence Berkley National Laboratory*, 1990. doi:10.2172/6660243

[4] P.L. Walstrom., "Soft-edged magnet models for higher-order beam-optics map codes", *Nucl. Instrum. Methods Phys. Res., Sect. A*, vol. 519, no. 1, pp. 216-221, 2004. doi:10.1016/j.nima.2003.11.158

[5] J.A. Nolen et al., "Design and Status of the Super Separator Spectrometer for GANIL SPRIAL2 Project", in *Proc. 12th International Conference on Heavy Ion Accelerator Technology* (HIAT 2012), Chicago, United States, June 2012, paper MOBO3. https://accelconf.web.cern.ch/HIAT2012/talks/mob03_talk.pdf

[6] D. Boutin et al., "Optical studies for the super separator spectrometer S3", in *Proc. 1st Int. Particle Accelerator Conf.* (IPAC 2010), Kyoto, Japan, May 2010, pp. 4464-4466, paper THPD079. http://hal.in2p3.fr/in2p3-00496346

[7] W. Wei et al., "Multipole magnets for the HIAF fragment separator using the Canted-Cosine-Theta (CCT) geometry", *J. Phys. Conf. Ser.* , vol. 1401, no. 1, pp. 1, 2020. doi:10.1088/1742-6596/1401/1/012015

[8] A.F. Zeller et al., "Magnetic elements for the A1900 fragment separator at the NSCL.", in *Advances in Cryogenic Engineering*, vol. 43, pp. 245-252, 1998. doi:10.1007/978-1-4757-9047-4_28